PHYSICAL REVIEW D **71,** 034019 (2005)

Quark self energy and relativistic flux tube model

Fabien Buisseret* and Claude Semay†

Groupe de Physique Nucléaire Théorique, Université de Mons-Hainaut, Académie universitaire Wallonie-Bruxelles, Place du Parc 20, B-7000 Mons, Belgium

(Received 24 December 2004; published 23 February 2005)

The contribution of the quark self energy to the meson masses is studied in the framework of the relativistic flux tube model. The equivalence between this phenomenological model and the more QCD based rotating string Hamiltonian is used as a guide to perform the calculations. It is shown that the addition of the quark self energy to the relativistic flux tube model preserves the linearity of the Regge trajectories. But, following the definition taken for the constituent quark masses, the Regge slope is preserved or decreased. In this last case, experimental data can only by reproduced by using a string tension around 0.245 GeV^2. Two procedures are also studied to treat the pure flux tube contribution as a perturbation of a spinless Salpeter Hamiltonian.

DOI: 10.1103/PhysRevD.71.034019 PACS numbers: 12.39.Pn, 12.39.Ki, 14.40.−n

I. INTRODUCTION

A successful way of understanding the properties of the mesons is to approximate the gluon exchanges between the quark and the antiquark by a string (the QCD string), characterized by its energy density, or tension. The relativistic flux tube model (RFTM) is a phenomenological model based on this picture [1,2]. More recently, the rotating string model (RSM) has been derived from the Nambu-Goto Lagrangian as an effective model which also describes a meson as a quark and an antiquark linked by a string [3,4]. The physical content of these models is very similar, and it has been shown that they are actually classically equivalent once the auxiliary fields appearing in the RSM are completely eliminated [5,6]. A rather good description of the experimental meson spectrum can be obtained with the original RFTM supplemented by a Coulomb term [7]. But unfortunately, a strong coupling constant larger than what it is expected from experimental analysis and lattice simulations must be considered. The necessity of finding new contributions arising from neglected physical mechanisms is thus clear. Recently, a quark self energy (QSE) contribution was introduced, which is due to the color magnetic moment of the quark propagating through the vacuum [8]. The QSE brings a negative contribution to the hadron masses, and seems to be an interesting way of reproducing the experimental data with a smaller Coulomb term.

Our purpose here is to study the influence of the QSE on the meson masses, especially using the RFTM. Our paper is organized as follows. Sec. II is a short presentation of both classical RFTM and RSM, where we also underline their classical equivalence. Since the equations describing these models are quite complicated, approximate equations are developed in Sec. III, from which an analytical mass formula is derived in Sec. IV. In Sec. V, the quality of the approximate equations are compared with the original quantized RFTM. We then introduce the QSE in Sec. VI and discuss its effects on the meson spectrum in Sec. VII. A comparison with experimental data is performed in Sec. VIII. Finally, some concluding remarks are outlined in Sec. IX.

II. ROTATING STRING AND RELATIVISTIC FLUX TUBE

We will present in this section two effective meson models: the rotating string model (RSM) and the relativistic flux tube model (RFTM). Our purpose is to give a presentation of the principal features of these models, and to underline their classical equivalence.

It has been shown in Ref. [3] that starting from the QCD Lagrangian, the Lagrange function of a meson can be built from the Nambu-Goto action. In first approximation the contributions due to the quark spins can be neglected. For two spinless quarks with masses m_1 and m_2, and a string with tension a, this action has the well-known form

$$\mathcal{L} = -m_1\sqrt{\dot{\boldsymbol{x}}_1^2} - m_2\sqrt{\dot{\boldsymbol{x}}_2^2} - a\int_0^1 d\beta\sqrt{(\dot{\boldsymbol{w}}\boldsymbol{w}')^2 - \dot{\boldsymbol{w}}^2\boldsymbol{w}'^2}. \tag{1}$$

In this action, $\boldsymbol{x}_i$ is the coordinate of quark i and $\boldsymbol{w}$ is the coordinate of the string. $\boldsymbol{w}$ depends on two variables defined on the string worldsheet: one is spacelike β and the other timelike τ. We have also defined $\boldsymbol{w}' = \partial_\beta \boldsymbol{w}$ and $\dot{\boldsymbol{w}} = \partial_\tau \boldsymbol{w}$. Introducing auxiliary fields (also known as einbein fields) to get rid of the square root in (1) and making the straight line ansatz to describe the string connecting the quark and the antiquark, an effective Hamiltonian can be derived, which reads [9]

*FNRS Research Fellow;
E-mail: fabien.buisseret@umh.ac.be
†FNRS Research Associate;
E-mail: claude.semay@umh.ac.be

 © 2005 The American Physical Society

$$H(\mu_i, \nu) = \frac{1}{2}\left[\frac{p_r^2 + m_1^2}{\mu_1} + \frac{p_r^2 + m_2^2}{\mu_2} + \mu_1 + \mu_2 + a^2 r^2 \int_0^1 \frac{d\beta}{\nu} + \int_0^1 d\beta \nu + \frac{L^2/r^2}{[\mu_1(1-\zeta)^2 + \mu_2\zeta^2 + \int_0^1 d\beta(\beta-\zeta)^2\nu]}\right]. \tag{2}$$

p_r is the common radial quark momentum. The parameter ζ defines the position $\boldsymbol{R}$ of the center of mass: $\boldsymbol{R} = \zeta \boldsymbol{x}_1 + (1-\zeta)\boldsymbol{x}_2$, and L is the orbital angular momentum of the system. The auxiliary fields μ_1 and μ_2 are seen as effective masses of the quarks whose current masses are m_1 and m_2. The last auxiliary field, ν, can be interpreted in the same way as an effective energy for the string whose "static" energy is ar. One can get rid of these auxiliary fields by a variation of the Hamiltonian (2). Their extremal values, denoted as μ_{i0} and ν_0, are the solutions of

$$\left.\frac{\delta H(\mu_i, \nu)}{\delta \mu_i}\right|_{\mu_i = \mu_{i0}} = 0, \tag{3a}$$

$$\left.\frac{\delta H(\mu_i, \nu)}{\delta \nu}\right|_{\nu = \nu_0} = 0. \tag{3b}$$

The equations of the RSM can be derived from the Hamiltonian (2) by the elimination of ν thanks to the condition (3b) [4]. We will consider in this paper the symmetrical case, where $m_1 = m_2 = m$ and $\mu_1 = \mu_2 = \mu$

$$\frac{L}{ar^2} = \frac{\mu y}{ar} + \frac{1}{4y^2}(\arcsin y - y\sqrt{1-y^2}), \tag{4a}$$

$$H^{\mathrm{RS}}(\mu) = \frac{p_r^2 + m^2}{\mu} + \mu + \frac{ar}{y}\arcsin y + \mu y^2. \tag{4b}$$

In the general case, where $m_1 \neq m_2$, a third equation has to be taken into account, which expresses the cancellation of the total momentum in the center of mass frame [6]. If one considers μ as a number, one can directly solve Eqs. (4) and find the meson mass, after a minimization of this mass with respect to μ [4].

Since the RSM equations contain the remaining auxiliary field μ and a variable y whose physical interpretation is not *a priori* clear, it appears interesting to go a step further and to get rid of μ. As it is shown in Ref. [5], the elimination of μ with the condition (3a) leads to the extremal value

$$\mu_0 = \sqrt{\frac{p_r^2 + m^2}{1-y^2}}. \tag{5}$$

Moreover, the replacement of μ by μ_0 in Eqs. (4) leads to the following expressions

$$\frac{L}{ar^2} = \frac{1}{ar} v_\perp \gamma_\perp W_r + f(v_\perp), \tag{6a}$$

$$H^{\mathrm{RS}}(\mu_0) = H^{\mathrm{RFT}} = 2\gamma_\perp W_r + ar\frac{\arcsin v_\perp}{v_\perp}, \tag{6b}$$

where we have defined

$$y = v_\perp, \quad \gamma_\perp = \frac{1}{\sqrt{1-v_\perp^2}},$$
$$f(v_\perp) = \frac{\arcsin v_\perp}{4v_\perp^2} - \frac{1}{4v_\perp\gamma_\perp} \quad \text{and} \tag{7}$$
$$W_r = \sqrt{p_r^2 + m^2}.$$

Eqs. (6) are precisely those of the RFTM as they appear in Ref. [1]. The mysterious variable y is now simply interpreted as the transverse velocity $v_\perp$ of the quarks, and the physical content of μ is clarified. Using definitions (7), we can rewrite (5) in the form

$$\mu_0 = W_r \gamma_\perp. \tag{8}$$

Originally, the RFTM was built on phenomenological arguments. But our derivation of the RFTM shows that it can be derived from the Nambu-Goto Lagrangian. We also clearly see the equivalence of the RSM and RFTM, when the auxiliary fields are eliminated. Let us note that this equivalence is also true in general, with $m_1 \neq m_2$ [6].

By application of the usual correspondence rules

$$p_r^2 \to -\frac{1}{r}\frac{\partial^2}{\partial r^2} r \quad \text{and} \quad L \to \sqrt{\ell(\ell+1)}, \tag{9}$$

the quantized equations of the RFTM are given by [1]

$$\frac{2\sqrt{\ell(\ell+1)}}{r} = \{v_\perp \gamma_\perp, W_r\} + a\{r, f(v_\perp)\}, \tag{10a}$$

$$H^{\mathrm{RFT}} = \{\gamma_\perp, W_r\} + \frac{a}{2}\left\{r, \frac{\arcsin v_\perp}{v_\perp}\right\}. \tag{10b}$$

The anticommutators $\{A, B\} = AB + BA$ arise because $v_\perp$, r, and p_r are non commuting operators. Let us note that the RFTM is not a covariant model. Models of this type, with square root operators for the kinetic energy, are generally referred to as semirelativistic. We keep here the name "Relativistic flux tube model" given in the original paper [1].

The quantized equations of the RSM, which are not used here, are given in Ref. [10]. The diagonalization of Hamiltonian H^{RFT} directly provides the physical masses M^{RFT}. Eqs. (10), as well as the quantized RSM ones, can be numerically solved, as it is done in Refs. [7,10]. After resolution, one observes that the quantized RFTM and RSM are no more equivalent, and lead to results which differ of about 10%. This is due to the auxiliary field μ, which is replaced by an operator in the RFTM, and treated like a number in the RSM (see Ref. [10]). This difference in the nature of the auxiliary field causes both models to be

nonequivalent in their quantized version. It has also been showed that, supplemented by an appropriate short range potential, like a Coulomb term, the quantized RFTM can rather well reproduce the meson spectra [7].

III. STRING AS A PERTURBATION

When $\ell = 0$, the RFTM reduces to a spinless Salpeter Hamiltonian (SSH) with a linear confinement potential ar [1]. If ℓ is small, the contribution of the string is also small, and then it can be treated as a perturbation of the SSH. We will show that the contribution of the string can be obtained by two different procedures, that lead to different definitions of the auxiliary field μ_0.

Let us start with the RSM and consider that the transverse velocity of the quarks is small: $y \ll 1$. We can develop formulas (4) at the second order in y. We obtain then

$$y^2 \approx \frac{\ell(\ell+1)}{r^2(ar/6+\mu)^2}, \tag{11a}$$

$$H^{\mathrm{RS}}(\mu) \approx \frac{p_r^2+m^2}{\mu} + \mu + ar + \left(\frac{ar}{6}+\mu\right)y^2. \tag{11b}$$

Inserting (11a) in (11b), and introducing $\vec{p}^2 = p_r^2 + \ell(\ell+1)/r^2$, we can write down an approximate Hamiltonian

$$H^{\mathrm{A}}(\mu) = \frac{\vec{p}^2+m^2}{\mu} + \mu + ar - \frac{a\ell(\ell+1)}{r\mu(6\mu+ar)}, \tag{12}$$

defining what we call here the perturbative flux tube model (PFTM). We see that $H^{\mathrm{A}}(\mu)$ is the sum of an usual SSH with linear confinement in the auxiliary field formalism [5]

$$H^{\mathrm{SS}}(\mu) = \frac{\vec{p}^2+m^2}{\mu} + \mu + ar, \tag{13}$$

and a specific contribution of the string, which reads

$$\Delta H_{\mathrm{str}}(\mu) = -\frac{a\ell(\ell+1)}{r\mu(6\mu+ar)}. \tag{14}$$

Since we want to treat $\Delta H_{\mathrm{str}}(\mu)$ as a perturbation, we will eliminate μ with the condition (3a) applied for the Hamiltonian $H^{\mathrm{SS}}(\mu)$. This leads to the extremal value

$$\mu_0 = \sqrt{\vec{p}^2+m^2}, \tag{15}$$

and after replacement in (13), to the spinless Salpeter Hamiltonian

$$H^{\mathrm{SS}} = 2\sqrt{\vec{p}^2+m^2} + ar. \tag{16}$$

Let us note that formula (15) is different from the extremal value (8). The string correction to compute is then given by [11]

$$\Delta M_{\mathrm{str}} = \langle \Delta H_{\mathrm{str}}(\mu_0)\rangle = -\frac{a\ell(\ell+1)\langle 1/r\rangle}{\langle\sqrt{\vec{p}^2+m^2}\rangle(6\langle\sqrt{\vec{p}^2+m^2}\rangle + a\langle r\rangle)}, \tag{17}$$

in which the mean value is performed with an eigenstate of H^{SS}. This string contribution was previously obtained in Ref. [11], where it is shown that its accuracy is better than 3%.

We can now invert the order of the operations: Firstly to eliminate μ in the RSM and obtain the RFTM, then make the same approximation as before. When $v_\perp \ll 1$, the RFTM equations can be developed at the second order in $v_\perp$ and we have

$$v_\perp \approx \frac{\sqrt{\ell(\ell+1)}}{r(W_r+\frac{ar}{6})}, \tag{18a}$$

$$H^{\mathrm{RFT}} \approx 2W_r + ar + v_\perp^2\left(W_r + \frac{ar}{6}\right). \tag{18b}$$

Replacing Eq. (18a) in Eq. (18b) leads to the Hamiltonian

$$\tilde{H}^{\mathrm{A}} = 2W_r + ar + \frac{\ell(\ell+1)}{r^2(W_r+ar/6)}. \tag{19}$$

Using the fact that

$$\sqrt{\vec{p}^2+m^2} = \sqrt{W_r^2 + \frac{\ell(\ell+1)}{r^2}}, \tag{20}$$

we can rewrite Hamiltonian (19) in the form

$$\tilde{H}^{\mathrm{A}} = 2\sqrt{\vec{p}^2+m^2} + ar + 2W_r - 2\sqrt{W_r^2 + \frac{\ell(\ell+1)}{r^2}} + \frac{\ell(\ell+1)}{r^2(W_r+ar/6)}. \tag{21}$$

Now, we make a new approximation and assume that $W_r \gg \sqrt{\ell(\ell+1)}/r$. In this case, which is justified in the limit $v_\perp \ll 1$, a first order expansion leads to

$$\sqrt{W_r^2 + \frac{\ell(\ell+1)}{r^2}} \approx W_r + \frac{\ell(\ell+1)}{2r^2W_r}. \tag{22}$$

With this approximation, we finally get from $\tilde{H}^{\mathrm{A}}$, a Hamiltonian with an usual form (a kinetic part with operator $\sqrt{\vec{p}^2+m^2}$)

$$H^{\mathrm{A}} = 2\sqrt{\vec{p}^2+m^2} + ar - \frac{a\ell(\ell+1)}{rW_r(6W_r+ar)}. \tag{23}$$

The approximate Hamiltonian (23) can again be seen as the sum of the Hamiltonian H^{SS} (16) and a contribution of the flux tube

$$\Delta H_{\mathrm{rft}} = -\frac{a\ell(\ell+1)}{rW_r(6W_r+ar)}. \tag{24}$$

As for formula (17), the flux tube contribution is given by

$$\Delta M_{\rm rft} = \langle \Delta H_{\rm rft} \rangle = -\frac{a\ell(\ell+1)\langle 1/r\rangle}{\langle\sqrt{p_r^2+m^2}\rangle(6\langle\sqrt{p_r^2+m^2}\rangle + a\langle r\rangle)}, \tag{25}$$

in which the mean value is again performed with an eigenstate of $H^{\rm SS}$. We immediately see that formulas (17) and (25) are different. In Sec. V, we will study the qualities of both corrections, but one can see that

$$\Delta H_{\rm str}(\mu_0) = \Delta H_{\rm rft} + \mathcal{O}[\ell^2(\ell+1)^2]. \tag{26}$$

Lets us note that the first contribution, proportional to $\ell^2(\ell+1)^2$, is a positive one.

IV. A MASS FORMULA

In the following, we will specially focus on the massless case, $m = 0$, for which we can expect the largest contributions of the flux tube (μ increases with the quark mass). In this case, it is possible to find an approximate analytical mass formula. This will allow a better understanding of the effects of the QSE (see Sec. VI C). Starting from the Hamiltonian (12), we define dimensionless conjugate variables $\vec{x}$ and $\vec{q}$ by the following scaling

$$\vec{r} = \frac{\vec{x}}{(\mu a)^{1/3}} \quad \text{and} \quad \vec{p} = (\mu a)^{1/3}\vec{q}. \tag{27}$$

In this section, we treat the auxiliary field μ as a number [8,11]. We can write the Hamiltonian (12) in the form

$$H^{\rm SS}(\mu) = \left(\frac{a^2}{\mu}\right)^{1/3}(\vec{q}^2 + x) + \mu, \tag{28}$$

with $x = |\vec{x}|$. Its eigenvalues are consequently

$$M^{\rm SS}_{n\ell}(\mu) = \left(\frac{a^2}{\mu}\right)^{1/3}\epsilon_{n\ell} + \mu, \tag{29}$$

where $\epsilon_{n\ell}$ is an eigenvalue of the Hamiltonian $(\vec{q}^2 + x)$, which is easy to solve numerically. Simple analytical approximate expressions of $\epsilon_{n\ell}$ can be found for ϵ_{n0} [5] and $\epsilon_{0\ell}$ [12]

$$\epsilon_{n0} \approx \left[\frac{3\pi}{4}\left(2n + \frac{3}{2}\right)\right]^{2/3}, \tag{30a}$$

$$\epsilon_{0\ell} \approx \frac{3}{2^{2/3}}\left(\ell + \frac{3}{2}\right)^{1/3}\left[\frac{\Gamma(\ell+2)}{\Gamma(\ell+3/2)}\right]^{2/3}. \tag{30b}$$

A more complicated approximate formula exists also in the general case [13].

Assuming that the quantities $\epsilon_{n\ell}$ are known, we can compute the extremal value of μ by a minimization of relation (29), which leads to

$$\mu_{0n\ell} = \sqrt{a}\left(\frac{\epsilon_{n\ell}}{3}\right)^{3/4}, \tag{31}$$

and

$$M^{\rm SS}_{n\ell}(\mu_{0n\ell}) = 4\mu_{0n\ell}. \tag{32}$$

We will now drop the explicit dependence in n and ℓ of the different terms to simplify the notations. When the flux tube contribution is added, the perturbation theory implies that the total energy is

$$M^{\rm A}(\mu_0) = 4\mu_0 - \frac{a\ell(\ell+1)}{\langle r\rangle\mu_0(6\mu_0 + a\langle r\rangle)}, \tag{33}$$

where $\langle 1/r\rangle$ is replaced by $1/\langle r\rangle$. The next step is to use the Hellmann-Feynman theorem [5,14], which states that

$$M^{\rm SS}(\mu_0) = 4\mu_0 = 2\mu_0 + a\langle r\rangle. \tag{34}$$

Extracting $\langle r\rangle$ from relation (34) and replacing it in relation (33), we finally obtain the mass formula

$$M^{\rm A}(\mu_0) \approx 4\mu_0 - \frac{a^2\ell(\ell+1)}{16\mu_0^3}, \tag{35}$$

where μ_0 is given by formula (31).

The mass formula (35), even approximate, exhibits Regge trajectories. This can be easily checked when $n = 0$. Using the fact that

$$\lim_{\ell\to\infty}\epsilon_{0\ell} \approx 3\left(\frac{\ell + 3/2}{2}\right)^{2/3}, \tag{36}$$

with formula (31), we obtain the following expression for the extremal value of the auxiliary field at large values of ℓ

$$\mu_0 \approx \sqrt{\frac{a\ell}{2}}. \tag{37}$$

Replacing Eq. (37) into Eq. (35), we get

$$[M^{\rm A}(\mu_0)]^2 \approx \frac{225}{32}a\ell. \tag{38}$$

This linear relation between the squared mass and the angular momentum reproduces qualitatively the Regge trajectories. The Regge slope is here $7.03a$, a higher value than the one predicted by the RFTM, which gives a slope equal to $2\pi a$ [1]. Finally, we can observe that

$$\lim_{\ell\to\infty}\frac{a^2\ell(\ell+1)/(16\mu_0^3)}{4\mu_0} = \frac{1}{16}. \tag{39}$$

When $\ell = 0$, this ratio is vanishing. This justifies to treat the contribution of the string as a perturbation.

V. COMPARISON BETWEEN EXACT AND APPROXIMATE STRING CONTRIBUTION

Before studying the contribution of the QSE to the RFTM, it is interesting to examine the relevance of the approximate treatment for the flux tube developed in Sec. III. For this purpose, we compare here some masses computed with the "exact" RFTM by numerically solving Eqs. (10), as it is done, for example, in Ref. [10], with masses computed in the framework of the PFTM with both string corrections (17) and (25).

The symbol M_E designs a mass computed with the RFTM, and M_{P1}, M_{P2} the corresponding PFTM masses evaluated with the string corrections (17) and (25), respectively. The quantities

TABLE I. $\Delta M_{E,P1}$ (correction (17)) in %, for different states, with $m = 0$. In this case, $\Delta M_{E,P1}$ is independent of a. ℓ is the orbital angular momentum of the state and n is the number of nodes at finite distance.

ℓ	1	2	3	4	5
$n = 0$	3.26	3.78	4.01	4.17	4.29
1	1.08	1.31	1.53	1.74	1.94
2	0.68	0.86	1.04	1.22	1.40
3	0.46	0.56	0.68	0.81	0.95
4	0.36	0.43	0.52	0.64	0.76
5	0.29	0.35	0.40	0.49	0.58

$$\Delta M_{E,Pi} = \left| \frac{M_E - M_{Pi}}{M_E} \right| \tag{40}$$

measure the differences between the RFTM and its approximations.

Table I presents the difference between the RFTM and the PFTM with correction (17). As the basis of the approximation was to consider a small $v_\perp$, it is not surprising to see that $\Delta M_{E,P1}$ increases with ℓ. On the contrary, $\Delta M_{E,P1}$ decreases for an increasing radial quantum number n. This can be understood by the presence of the operator p_r^2 in the denominator of Eq. (17). This term becomes larger with n, and makes the contribution of the string smaller, leading to a decreasing of $\Delta M_{E,P1}$. Globally, the approximation considered in Table I is rather good, in particular, when $n \geq \ell$.

Table II presents the difference between the RFTM and the PFTM with correction (25). When $n = 0$, we immediately see that this approximation is not so good, because $\Delta M_{E,P2}$ becomes large very quickly with ℓ. As in Table I, the situation is better for larger values of n, when our approximation $W_r \gg \sqrt{\ell(\ell+1)}/r$ is particularly justified. This is also due to the presence of the operator p_r^2 in the denominator of Eq. (25). But the evolution is less monotonic than in Table I. In particular, for a fixed value of n, $\Delta M_{E,P2}$ decreases to a minimal value, and then increases again with ℓ.

In the framework of the PFTM, the correction (17), proposed in Ref. [11], which contains all orders in $\ell(\ell+1)$ (see Eq. (26)), seems preferable since it provides quite globally good results. Let us mention that, in the framework of the RFTM, the operator W_r arises naturally instead of the operator $\sqrt{\vec{p}^2 + m^2}$. The bad results obtained with the correction (17) are due to the necessity to perform the approximation $W_r \gg \sqrt{\ell(\ell+1)}/r$, in order to obtain a Hamiltonian with an usual form, that is to say an usual kinetic part.

TABLE II. Same as in Table I but for $\Delta M_{E,P2}$ (correction (25)).

ℓ	1	2	3	4	5
$n = 0$	1.03	7.81	15.21	22.52	29.54
1	0.44	0.88	2.55	4.41	6.36
2	0.40	0.67	0.73	1.62	2.64
3	0.35	0.14	0.23	0.72	1.30
4	0.31	0.19	0.02	0.30	0.66
5	0.26	0.19	0.06	0.13	0.37

VI. THE QUARK SELF ENERGY

A. Definition

Recently, it was shown that the QSE contribution, which is created by the color magnetic moment of the quark propagating through the vacuum background field, adds a negative constant to the hadron masses [8]. Its negative sign is due to the paramagnetic nature of the particular mechanism at work in this case. Other contributions due to quark spin (spin-spin, spin-orbit) also exist but they are smaller that the QSE one [3], and they are neglected in this work. Using the Fock-Feynman-Schwinger representation of the quark Green's function, one can obtain the QSE contribution as a shift of the squared mass of the quark [8,15] which reads

$$\Delta m^2 = -3m \int_0^\infty dz\, z^2 K_1(mz)[D(z) + D_1(z)], \tag{41}$$

where D and D_1 are quark correlators and K_1 the MacDonald function. The properties of these correlators were studied by lattice simulations in the quenched case [16]. One has then

$$D(z) \approx 3D_1(z) = D(0)\exp(-|z|\delta), \tag{42}$$

with $\delta = 1/T_g$. T_g is the gluonic correlation length, whose value is estimated at about 0.15–0.2 fm. This locates δ in the interval 1.0–1.3 GeV. The results (42) allow us to find an analytic form for the integral (41)

$$\Delta m^2 = -4mD(0)\varphi(m/\delta), \tag{43}$$

where, defining $\epsilon = m/\delta$, we can write $\varphi(\epsilon)$ as

$$\varphi(\epsilon) = \begin{cases} \frac{1}{\delta^3}\left[\frac{-3\epsilon}{(1-\epsilon^2)^{5/2}} \ln\left(\frac{1+\sqrt{1-\epsilon^2}}{\epsilon}\right) + \frac{1+2\epsilon^2}{\epsilon(1+\epsilon^2)^2}\right] & = \frac{1}{\delta^3}\phi_1(\epsilon)(\epsilon < 1) \\ \frac{1}{\delta^3}\left[\frac{-3\epsilon}{(\epsilon^2-1)^{5/2}} \arctan(\sqrt{\epsilon^2 - 1}) + \frac{1+2\epsilon^2}{\epsilon(1-\epsilon^2)^2}\right] & = \frac{1}{\delta^3}\phi_2(\epsilon)(\epsilon > 1). \end{cases} \tag{44}$$

One can check that $\phi_1(1) = \phi_2(1) = 2/5$, and that

$$\lim_{\epsilon\to 0}\phi_1(\epsilon) = \frac{1}{\epsilon}. \tag{45}$$

For a purely exponential correlator, as it is the case here, $D(0)$ is connected with the string tension a by the relation

$$a = \frac{1}{2}\int d^2xD(x) = \frac{\pi D(0)}{\delta^2}, \tag{46}$$

so we find

$$\Delta m^2 = -\frac{4am\delta^2}{\pi}\varphi(\epsilon). \tag{47}$$

For convenience, we define a new dimensionless function, $\eta(\epsilon)$, by

$$\eta(\epsilon) = \delta^3\epsilon\varphi(\epsilon). \tag{48}$$

We see in Fig. 1 that $\eta(0) = 1$ and that $\eta(\epsilon)$ rapidly decreases for increasing values of ϵ.

Thanks to the definition (48), Eq. (47) takes its final form [8]

$$\Delta m^2 = -\frac{4a}{\pi}\eta(\epsilon). \tag{49}$$

An important ingredient we have used to get the contribution (49) of the QSE is the relation (42), derived in the quenched case. In Ref. [15], the results obtained in the unquenched case are quite different: the exponential form of D remains the same, but now D_1 is small enough to be neglected. This approximation leads us, after the same calculations as before, to

$$\Delta m^2 = -\frac{3a}{\pi}\eta(\epsilon). \tag{50}$$

The two formulas (49) and (50) only differ by a constant factor: 4 in the quenched case, 3 in the unquenched one. Since this factor does not seem to be presently known with a great accuracy, we will finally use the following expression for the quark self energy

$$\Delta m^2 = -\frac{fa}{\pi}\eta(m/\delta), \tag{51}$$

with $f \in [3, 4]$ and $\delta \in [1.0, 1.3]$ GeV.

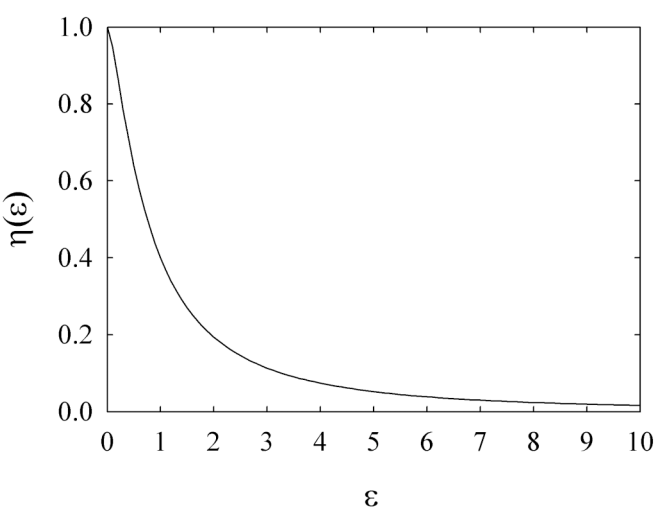

FIG. 1. Plot of $\eta(\epsilon)$.

B. Insertion of QSE in effective meson models

In the previous section, we showed how the QSE contribution acts as a shift of the squared mass of the quarks. We now have to insert this new term in the models we described in Secs. II and III. If we make the substitution $m_i^2 \to m_i^2 + \Delta m_i^2$ in the Hamiltonian (2), we find

$$H \to H + \Delta H_{\rm QSE}, \tag{52}$$

where

$$\Delta H_{\rm QSE} = \sum_{i=1}^{2}\frac{\Delta m_i^2}{2\mu_i} = -\frac{fa}{\pi}\sum_{i=1}^{2}\frac{\eta(m_i/\delta)}{2\mu_i}. \tag{53}$$

Eq. (53) is the total contribution of the QSE to the RS Hamiltonian. This term has to be considered as a perturbation of the original Hamiltonian, and thus one has not to give much sense to the fact that for light quarks the total mass $m^2 + \Delta m^2$ is negative [8]. Since the QSE is a perturbation of the Hamiltonian, it has not to be included in the elimination of the auxiliary field μ. To take into account the QSE in the RFTM, we suggest the following procedure, inspired from Ref. [8]:

(1) To find the eigenvalues and eigenfunctions of the RFTM Hamiltonian.
(2) To compute the mean value $\langle\mu_0\rangle$ of the extremal field μ_0 with the eigenfunctions.
(3) To add to each eigenvalue the corresponding QSE contribution (53) which reads, in the symmetrical case,

$$\Delta M_{\rm QSE} = -\frac{fa}{\pi}\frac{\eta(m/\delta)}{\langle\mu_0\rangle}. \tag{54}$$

The problem is to choose the value μ_0 of the extremal field. Within the PFT, this value is given by Eq. (15), and the resulting QSE correction is given by

$$\Delta M_{\rm QSE}^{\rm PFT} = -\frac{fa}{\pi}\frac{\eta(m/\delta)}{\langle\sqrt{\vec{p}^2 + m^2}\rangle}, \tag{55}$$

as it is done in Ref. [11]. On the other hand, if the equations of the RFTM are not treated in perturbation, it seems natural to take $W_r\gamma_\perp$ for μ_0 (see Sec. II). Within this framework, the QSE contribution is expected to be given by

$$\Delta M_{\rm QSE}^{\rm RFT} = -\frac{fa}{\pi}\frac{\eta(m/\delta)}{\langle W_r\gamma_\perp\rangle}. \tag{56}$$

Actually, we have to replace $W_r\gamma_\perp$ by $\{W_r, \gamma_\perp\}/2$ in order

to keep the operator hermitian. We can expect that both procedures will lead to different results, as in the case of the contribution of the string as a perturbation (see Sec. III). But the situation is somewhat different since no approximation of type $v_\perp \ll 1$ is needed to obtain Eq. (56). Moreover, both operators $\sqrt{\vec{p}^2 + m^2}$ and $W_r\gamma_\perp$ contain all orders in $\ell(\ell+1)$. A first order expansion allows to have an idea of the differences between both approaches

$$\sqrt{\vec{p}^2 + m^2} \approx W_r + \frac{\ell(\ell+1)}{2W_r r^2}, \tag{57a}$$

$$W_r\gamma_\perp \approx W_r + \frac{\ell(\ell+1)}{2W_r r^2}\frac{1}{(1 + ar/6W_r)}. \tag{57b}$$

Relation (57b) can be obtained only if we assume $v_\perp \ll 1$.

C. Regge trajectories

As mentioned in Ref. [8], the QSE correction preserves the Regge trajectories. We can qualitatively understand this thanks to the mass formula (35), to which we add the QSE contribution (53). We have

$$M^{\mathrm{A}}(\mu_0) = 4\mu_0 - \frac{a\ell(\ell+1)}{16\mu_0^3} - \frac{fa}{\pi}\frac{\eta(m/\delta)}{\mu_0}. \tag{58}$$

For large angular momentum, μ_0 becomes large. Keeping only the dominant terms, we find the approximate mass formula

$$[M^{\mathrm{A}}(\mu_0)]^2 \approx 16\mu_0^2 - 8\frac{fa}{\pi}\eta(m/\delta). \tag{59}$$

It appears that the Regge trajectories are preserved, since the QSE only causes a global shift of the squared masses and preserves the dominant $16\mu_0^2$ term, which grows like ℓ. This is particularly clear when $n = 0$ (see Eq. (37)).

VII. ADDING THE QSE

In this section, we compute numerically the contributions of the QSE for both the RFTM and the PFTM. We will focus on the massless case, for which we expect the largest effect since $\eta(0) = 1$ and the extremal field μ_0 is minimal. In this special case, we are able to perform a universal analysis of our results, since the meson masses are then just scaled by the factor $\sqrt{a}$. We will use in this section $f = 3.0$, which is the value computed in the unquenched case.

We noticed in Sec. VI C that adding the QSE contribution did not destroy the Regge trajectories and the Regge slope. This result was obtained using a mass formula, itself an approximation of the PFTM. Since we are able to numerically solve the RFTM without making approximations [10], we can directly study the influence of the QSE correction on the Regge trajectories. The main graph of Fig. 2 immediately shows the negative shift of the squared masses when the QSE is added, as expected. If the linearity

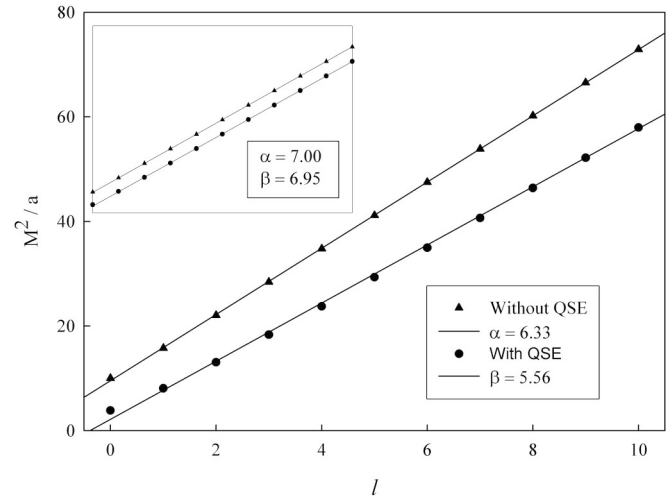

FIG. 2. Main: Regge trajectories for $n = 0$ with (circle) and without (triangle) QSE, computed with the RFTM. Small box: Same Regge trajectories computed with the PFTM. Lines are used to guide the eyes.

of the Regge trajectories is well preserved with the RFTM, the Regge slope is not. In this figure, β is the Regge slope with QSE and α is the corresponding one without QSE. Both are rather different, and we obtain $\beta/\alpha = 0.88$. This diminution of the slope is caused by the QSE term (56). The small box shows that when one is working with the PFTM and the QSE term (55), as it is the case in [11], the Regge slope is not affected, or a very little bit. We find indeed $\beta/\alpha = 0.99$.

We now have to understand why the QSE affects the Regge slope in the RFTM and not in the PFTM. Figure 3 illustrates the differences between the QSE contributions (55) and (56). When $\ell = 0$ both contributions are equal

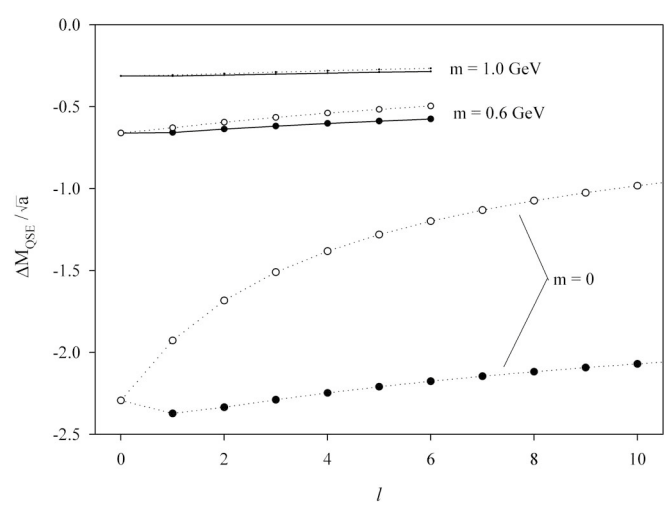

FIG. 3. QSE contributions, for $n = 0$, versus ℓ. The QSE contributions in the RFTM (filled circle) and with the PFTM (open circle) are computed for different quark masses. Note that when $m \neq 0$, the scaled results are not independent of a, which is taken here equal to 0.19 GeV^2.

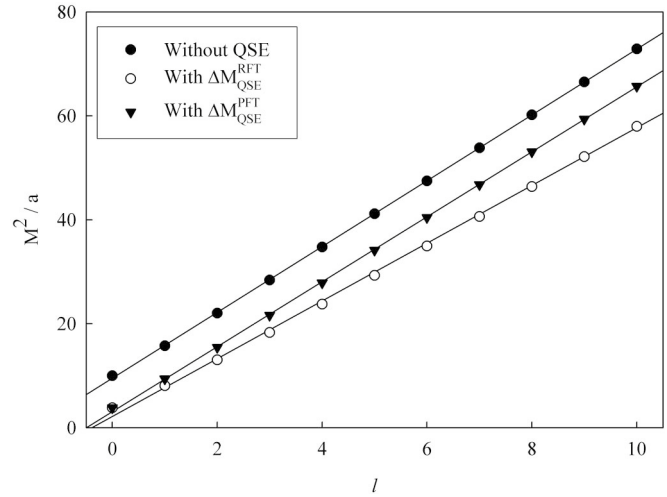

FIG. 4. Regge trajectories, with $n = 0$, for the genuine RFTM (filled circle), the RFTM with a theoretically expected QSE term $\Delta M^{\rm RFT}_{\rm QSE}$ (open circle) and with a QSE term inspired by the PFTM $\Delta M^{\rm PFT}_{\rm QSE}$ (triangle).

since the PFTM and the RFTM reduce to the same spinless Salpeter equation. In the massless case, the two contributions considerably differ for $\ell \neq 0$. The QSE coming from the RFTM is always the smaller one, and this causes the Regge slope to be smaller when one solves the RFTM. As expected, the difference between the two contributions decreases when the quark mass increases. With a large quark mass, both RFTM and PFTM have a common non relativistic limit (when the approximation $v_\perp \ll 1$ is the most justified). We could expect from Eq. (57) that $\langle W_r \gamma_\perp \rangle$ is approximately equal to $\langle \sqrt{\vec{p}^2 + m^2} \rangle$, but Fig. 3 shows that for light quarks this is not verified. We show in Fig. 4 the effect of adding to the RFTM solutions a "theoretically justified" QSE term (56) and a "PFTM-like" one (55). As expected, the contribution (55) causes no diminution of the Regge slope.

VIII. EXPERIMENTAL DATA

Realistic meson masses cannot be computed with the genuine flux tube Hamiltonian (10b). It can indeed give the right Regge slope with $a \lesssim 0.2$ GeV, but the absolute values of the masses are always too high. An attractive Coulomb potential, simulating the one-gluon exchange process, must be added

$$V(r) = -\frac{4}{3}\frac{\alpha_S}{r}, \tag{60}$$

where α_S is the strong coupling constant. Using the technique of Sec. IV, the contribution of this potential is

$$\langle V(r) \rangle \approx -\frac{4}{3}\frac{\alpha_S}{\langle r \rangle} = -\frac{4}{3}\frac{\alpha_S a}{2\mu_0}, \tag{61}$$

in first order perturbation theory. Formula (35) implies that this contribution to the Regge trajectory is a simple shift in square mass given by $-16\alpha_S a/3$.

The coupling constant α_S has, in principle, a r-dependence and several forms are possible (see for instance Refs. [7,17,18]). In this work, we focus only on light quark systems because the largest differences between the two QSE terms studied here are expected for such systems. Only mesons containing heavy quarks have an enough small radius to probe the very short range part of the interaction, where α_S deviates strongly from a constant. As we are only interested in the main features of the meson spectra, we use here a fixed value for α_S.

Theoretical arguments as well as lattice calculations agree with a value $\alpha_S \leq 0.4$ [19]. However, even such a Coulomb term does not shift the masses enough to reproduce the data (see, for example, Ref. [7]), except if unrealistic too high values are chosen for α_S. This means that other contributions coming from neglected physical mechanisms are still needed. The QSE seems to be an interesting one, because its contribution to the mass is negative, and rather large. This should allow to reproduce the experimental data with an acceptable value for the Coulomb term.

In Table III, we give the two sets of parameters we use to compute the masses of some $n\bar{n}$ states. Both have the same value δ and α_S but differ for the other parameters. We have checked than the masses of light mesons decrease by less than 1% when δ increases from one to 1.3 GeV (the meson mass variation with δ vanishes when $m = 0$ since the η function depends only on m/δ).

In the type 1, we make the usual choice $m_n = 0$ and take formula (56) as QSE term. This is the contribution that one can theoretically expect. As we have seen that it causes a diminution of the Regge slope, we have to take $a = 0.245$ GeV^2 in order to obtain a final slope in agreement with the experiment. Choosing $a = 0.2$ GeV^2 is no longer possible as it is the case with the PFTM [11]. This is the unconventional aspect of type 1 set of parameters. On the other side, with the type 2 set, it is possible to keep for a the standard value, about 0.2 GeV^2. The price to pay is to take formula (55) as QSE term, an only "empirically" justified choice, and to give a mass to the quark n. The value of 73 MeV can seem high, but it is smaller than constituent

TABLE III. Two sets of possible physical parameters.

	Type 1	Type 2
a(GeV^2)	0.245	0.195
m_n (GeV)	0.0	0.073
α_S	0.4	0.4
f	3.2	3.0
δ (GeV)	1.0	1.0
QSE term	$\Delta M^{\rm RFT}_{\rm QSE}$	$\Delta M^{\rm PFT}_{\rm QSE}$

TABLE IV. Comparison between the spin averaged masses $M_{\rm av}$ of the $n\bar{n}$ states and the results of the RFTM plus a QSE term. M_1 and M_2 are the masses computed with the set of parameters 1 and 2, respectively. Masses are given in GeV. The first three columns show the different states used to compute the spin averaged masses.

State	I	$(n+1)^{2S+1}L_J$	$M_{\rm av}$	M_1	M_2
ω	0	1^3S_1	0.773 ± 0.011	0.787	0.775
ρ	1	1^3S_1			
$h_1(1170)$	0	1^1P_1	1.265 ± 0.011	1.269	1.284
$b_1(1235)$	1	1^1P_1			
$f_1(1285)$	0	1^3P_1			
$a_1(1260)$	1	1^3P_1			
$f_2(1270)$	0	1^3P_2			
$a_2(1320)$	1	1^3P_2			
$\omega(1650)$	0	1^3D_1	1.676 ± 0.012	1.673	1.678
$\rho(1700)$	1	1^3D_1			
$\omega_3(1670)$	0	1^3D_3			
$\rho_3(1690)$	1	1^3D_3			
$f_4(2050)$	0	1^3F_4	2.015 ± 0.012	2.016	2.006
$a_4(2040)$	1	1^3F_4			

masses, around 200–300 MeV, generally used in some potential models. Moreover, a good agreement with data can still be obtained with a smaller value of m_n and a slightly larger value for a.

The comparison between the experimental masses and our results is given in Table IV. Since the RFTM includes neither the spin (S) nor the isospin (I) of the mesons, the experimental data we will try to reproduce here are the spin and isospin averaged masses, denoted $M_{\rm av}$. These are given by [17]

$$M_{\rm av} = \frac{\sum_{I,J}(2I+1)(2J+1)M_{I,J}}{\sum_{I,J}(2I+1)(2J+1)}, \tag{62}$$

with $\vec{J} = \vec{L} + \vec{S}$ and $M_{I,J}$ are different masses of the states with the same orbital angular momentum ℓ. The first three columns of Table IV show the experimental data concerning $n\bar{n}$ (n means u or d) states used to compute the spin-isospin averaged masses. These data are taken from Ref. [20]. We see that both models lead to masses close to the spin-isospin averaged ones, our results being located inside the error bar in almost every case.

IX. CONCLUDING REMARKS

The purpose of this work was to study the contribution of the quark self energy to the meson masses in the framework of the relativistic flux tube model. The equivalence between this phenomenological model and the more QCD based rotating string Hamiltonian is used as a guide to perform the calculations.

The equations defining the relativistic flux tube model being rather complicated to solve, it seems interesting to treat the flux tube contribution as a perturbation. Two procedures have been studied. To eliminate firstly the auxiliary field from the rotating string Hamiltonian, or to make firstly the approximation of small transverse velocities in the rotating string Hamiltonian. We arrived in Sec. III at two non equivalent terms for the flux tube correction: the first one, obtained in the auxiliary field formalism, was already known [11], and the second one, obtained directly from the relativistic flux tube equations, which can be considered as the zero order expansion in $\ell(\ell+1)$ of the first one. The results of both contributions are quite similar, but we showed in Sec. V that the first approach is globally the best one.

Starting from the rotating string Hamiltonian and considering the auxiliary field associated with the quark mass μ as a simple number, an approximate but analytical mass formula is established. It enables to understand at least qualitatively why the quark self energy preserves the linearity of the Regge trajectories and decreases the squared masses by a constant quantity (see Secs. IV and VI C).

The addition of the quark self energy to the relativistic flux tube model (Sec. VII) preserves the linearity of the Regge trajectories. But, for massless quarks, the Regge slope is smaller by a factor 0.88 with the quark self energy than without it (this value tends toward unity when the quark masses increase). This effect does not exist when one works within the framework of a perturbation theory, in which the relativistic flux tube Hamiltonian reduces to a spinless Salpeter Hamiltonian. It is due to the fact that different extremal values of the field μ are found, $\sqrt{\vec{p}^2 + m^2}$ or $W_r\gamma_\perp$, considering the perturbation scheme or not.

In the framework of the relativistic flux tube model, it is possible to reproduce the experimental data with the theoretically expected quark self energy term ($\mu = W_r\gamma_\perp$) and a realistic Coulomb term, if a larger value than usual, 0.245 GeV^2, is chosen for the string tension a. As the value of Regge slope is mainly determined by this parameter, it is not possible to use a smaller value of a by changing the values of the other parameters α_S or δ. On the contrary, the usual value $a = 0.2$ GeV^2 can be used by choosing a quark self energy term coming from a perturbation approach ($\mu = \sqrt{\vec{p}^2 + m^2}$).

We believe that the quark self energy term in which the extremal field μ is given by $W_r\gamma_\perp$ must be used, because it is the natural value associated with the relativistic flux tube model. But, in this case, the value of the string tension must be around 0.245 GeV^2. We expect that the use the usual value 0.2 GeV^2 is possible if some physical mechanisms neglected in this study (spin contributions, retardation effects) are taken into account. More exotic phenomena, like deviations from the straight line for the flux tube, are also possible. Such a work is in progress.

[1] D. LaCourse and M. G. Olsson, Phys. Rev. D **39**, 2751 (1989).
[2] M. G. Olsson and S. Veseli, Phys. Rev. D **51**, 3578 (1995).
[3] A. Yu. Dubin, A. B. Kaidalov, and Yu. A. Simonov, Phys. At. Nucl. **56**, 1745 (1993); [Yad. Fiz. **56**, 213 (1993).]
[4] V. L. Morgunov, A. V. Nefediev, and Yu. A. Simonov, Phys. Lett. B **459**, 653 (1999).
[5] C. Semay, B. Silvestre-Brac, and I. M. Narodetskii, Phys. Rev. D **69**, 014003 (2004).
[6] F. Buisseret and C. Semay, Phys. Rev. D **70**, 077501 (2004).
[7] C. Semay and B. Silvestre-Brac, Phys. Rev. D **52**, 6553 (1995).
[8] Yu. A. Simonov, Phys. Lett. B **515**, 137 (2001).
[9] E. L. Gubankova and A. Yu. Dubin, Phys. Lett. B **334**, 180 (1994).
[10] F. Buisseret and C. Semay, Phys. Rev. E (to be published).
[11] A. M. Badalian and B. L. G. Bakker, Phys. Rev. D **66**, 034025 (2002).
[12] W. Lucha and F. F. Schöberl, Phys. Rev. A **51**, 4419 (1995).
[13] S. K. Bose, A. Jabs, and H. J. W. Müller-Kirsten, Phys. Rev. D **13**, 1489 (1976).
[14] R. P. Feynman, Phys. Rev. **56**, 340 (1939).
[15] A. Di Giacomo and Yu. A. Simonov, Phys. Lett. B **595**, 368 (2004).
[16] A. Di Giacomo and H. Panagopoulos, Phys. Rev. B **285**, 133 (1992).
[17] F. Brau and C. Semay, Phys. Rev. D **58**, 034015 (1998).
[18] C. Semay and B. Silvestre-Brac, Nucl. Phys. A **647**, 72 (1999).
[19] Yu. A. Simonov, JETP Lett. **57**, 525 (1993).
[20] Particle Data Group, S. Eidelman *et al.*, Phys. Lett. B **592**, 1 (2004).